The Syphon Bubble Reactor Heat Transformer as Heatpump in the REHOS cycle

by
Johan Enslin

Heat Recovery Micro Systems

Heidelberg
South Africa

Abstract:

The REHOS Power cycle is really a combination of two sub-cycles, namely a Heat Transformer type heat pump, coupled regeneratively to an Organic Rankine Power cycle (ORC). The ORC is a well developed and commercially attractive technology used in various waste heat recovery applications worldwide. The operation of the absorption heat transformer (AHT) type heat pumps, even though several are used commercially, are less well known, and are described in this paper to emphasize some very interesting aspects of heat powered heatpumps.

A very efficient novel low temperature heat transformer type heatpump, called the Syphon Bubble Reactor Heat Transformer (Syphon-BRHT) is described and the detailed design shared. This heatpump would be of tremendous commercial value for use as heat pump for the upgrade of low temperature waste heat, as well as utilization of the primary heat pump sub-cycle for the highly efficient REHOS Power cycle. It's simplicity and high heat load capability makes it extremely attractive from a commercial point of view.

The described Syphon-BRHT heatpump is in the process of being constructed using the design information as presented in this paper.

Introduction:

The Regenerative Heat of Solution (REHOS) thermodynamic cycle basically consist of two sub-cycles, coupled regeneratively. An Absorption Heat Transformer (AHT) type heat pump as primary sub-cycle, provide the pumped (upgraded) heat to an Organic Rankine Cycle (ORC) that produce power from it (power sub-cycle). The heat rejected from the ORC is regeneratively re-used as partial input, low temperature (degraded) waste heat by the heat pump, with the addition of a small portion external waste heat (or ambient heat from the environment) upgraded by the heat pump.

The technology of the Organic Rankine Cycle (ORC) is well understood and the production of power from waste heat is widely used commercially. A very simple example diagram of an ORC highlighting the high temperature evaporator heat exchanger as well as the cold condenser heat rejection heat exchanger is represented in Figure 1.

Figure 1

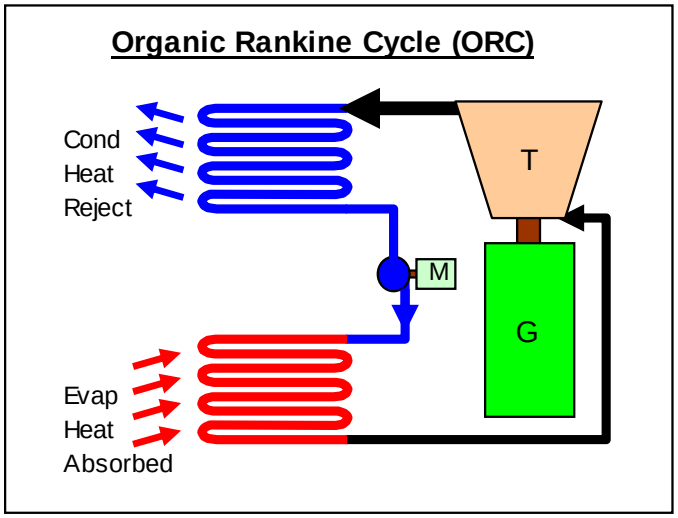

This power sub-cycle of the REHOS thermodynamic cycle -elaborated on in a previous publication [9], among others, therefore need no further discussion. It represent a mature, well developed technology. We may therefore focus explanations and descriptions on the heat pump primary sub-cycle of the REHOS.

We have already compared various heat pump technologies and published the paper [19] on the subject, already concluding that the only economically viable type of heat pump to use as primary sub-cycle in the REHOS cycle would have to be mainly heat powered, with the minimum electricity used, as the electricity used would subtract from the REHOS power output, decreasing efficiency. The electrical energy required by vapor compression (VC) type heat pumps are simply prohibitively high. The absorption heat transformer (AHT) have therefore been investigated for use in the REHOS cycle. The convention for heatpump efficiency calculations (Coefficient of Performance or COP) have also been dealt with in the publication [18].

The difference between the absorption heat pump (refrigerator) and the AHT have been detailed in the introduction of the REHOS concepts in the international conference [12] published July 2017 and have been re-iterated a few times in other publications. The AHT demonstrate the upgrading of intermediate temperature heat to higher temperatures, making use of the heat of solution (HOS) released when certain liquids mix (or un-mix) like ammonia and water (NH3 in aqua) to form zeotropic mixtures.

The regenerative coupling of the two sub-cycles (Heat pump and ORC) to form the REHOS cycle is demonstrated simplistically in the schematic of figure 2, below. Higher temperature heat delivered by the heat pump is used for the ORC evaporator heat exchanger, and the ORC heat rejection condenser heat exchanger coil deliver the low temperature vapor condensing heat as waste heat source for the heat pump heat input. This waste heat source must be supplemented with a portion additional input heat to achieve overall heat balance of the REHOS cycle.

Figure 2

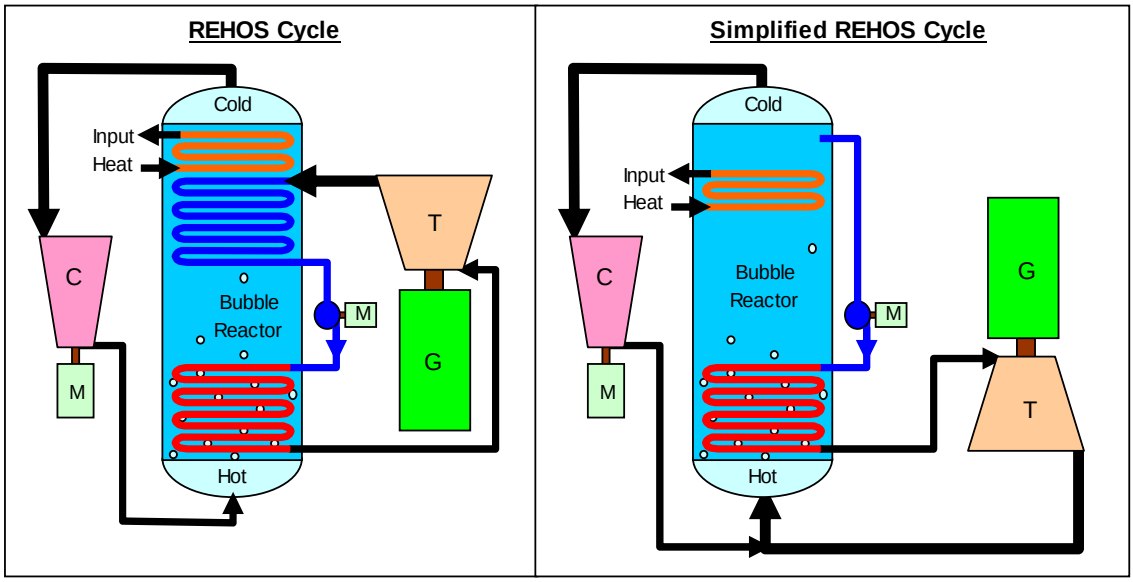

In our quest for the ideal AHT type heat pump for use in the REHOS cycle, let us have a re-look at the current state-of-the-art. The simple AHT is sketched on a Log-Pressure vs Temperature line diagram as per figure 3, below. This represent the commercial thermodynamic cycle used eg. by Rivera [3] for the commercial upgrade of heat from a traditional Solar Pond.

Notice that some intermediate temperature heat (Qde) is used to release vapor in the desorber, and this latent heat must be rejected again in the condenser (Qco) to liquefy this vapor for pumping. This type of mechanism for generating the required liquid to be pumped to the evaporator is therefore quite wasteful in energy utilization. It does use heat, however, to power the waste heat temperature upgrade, as the liquid pump energy requirement is at least two orders of magnitude smaller than the heat flow, and can therefore generally be ignored.

Figure 3

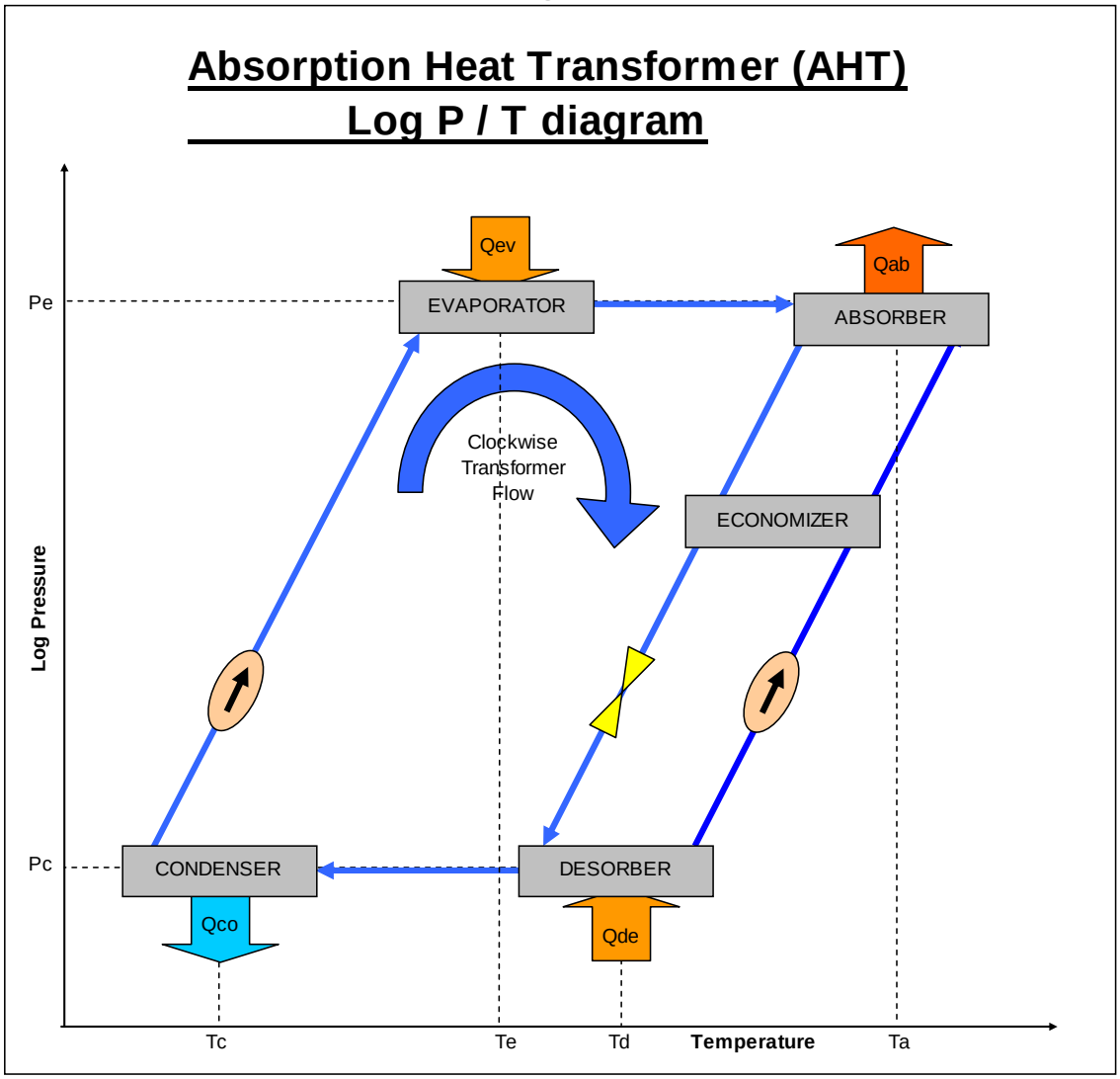

The AHT sketched in figure 3 represent the norm for heat powered waste heat temperature upgrading, but over the years it has been adapted in various ways. The Sliding Temperature AHT Hybrid heat pump sketched as Log-P vs Temperature in figure 4, below, is one such example. This type of heat pumps also allow sliding temperature heat source and sink, allowing operation on the high efficiency Lorenz cycle. This was extensively elaborated on by Jensen [4]. In this cycle, both the desorber and absorber operate at their own fixed pressures, but sliding temperatures brought about by ammonia concentration changes (in the NH3 in aqua zeotropic binary mixture in the heat exchangers). This allow by way of an example, the desorber (as well as the absorber) to operate at fixed pressure, but the local temperature in the heat exchanger following the decreasing temperature of the liquid being cooled as heat source (or heated in the absorber).

The use of this Lorenz cycle principles was seriously elaborated on in papers handling the development of the Kalina cycle, like Kiesela et al [6] published already in 1996, as well as development of the Hybrid Absorption Heat Pump Process [5] by Borgås in his Master's thesis. Other principles of zeotropic binary liquid mixtures are also covered in the thesis of Govindaraju [9] published 2005, while the IEA Handbook on thermally driven heat pumps [2] published in 2013 provide valuable insight into calculation conventions and standards for heat pumps used commercially.

Figure 4

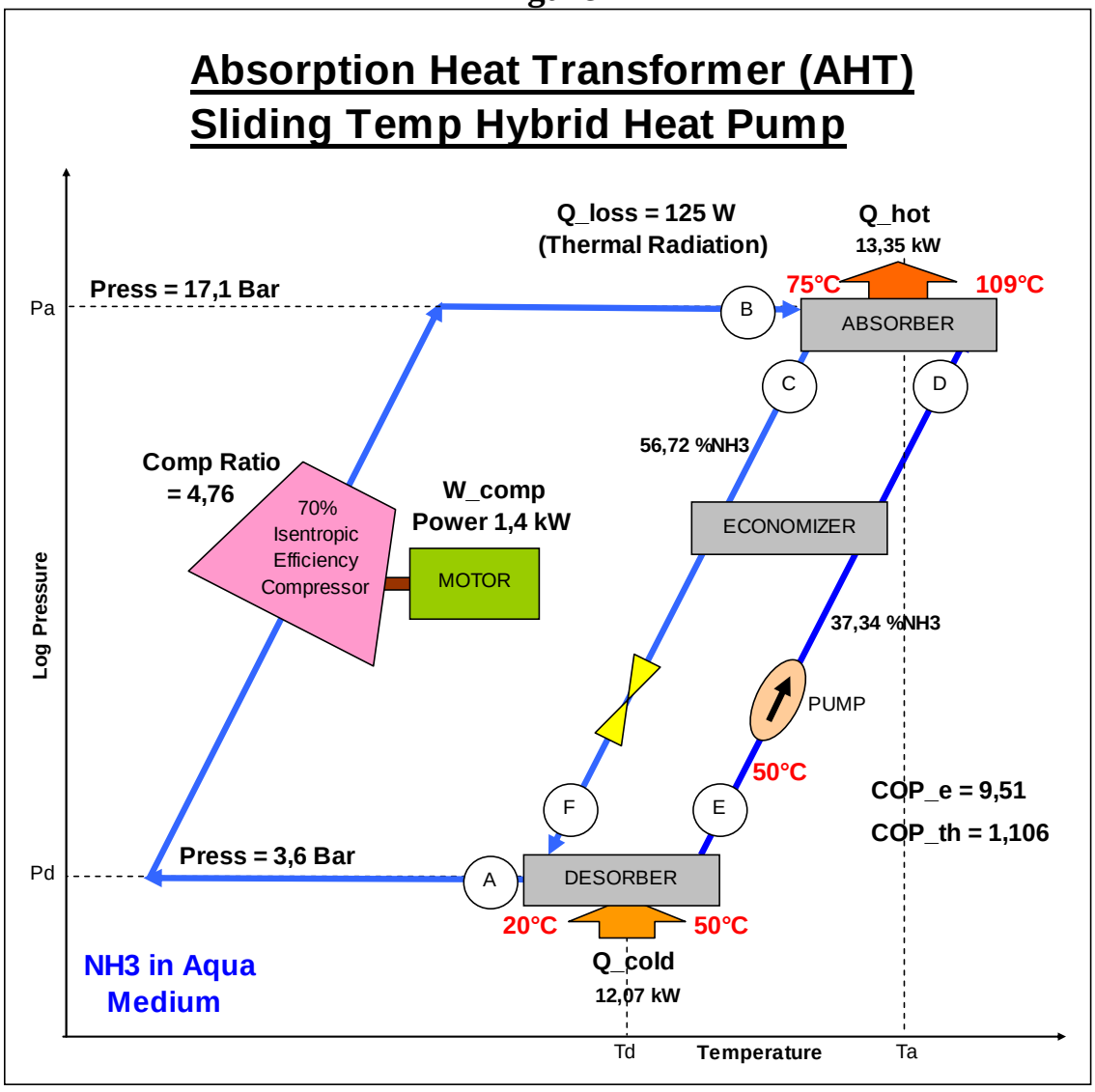

The Log-P vs Temperature diagram in figure 4 have been discussed in detail in the publication [19], but it is redrawn here to emphasize certain aspects of the Heat Transformer. The most important aspect of all AHT type heat pumps, must be the demonstration that vapor, even if it is generated at a low temperature, may be used as transfer medium to generate higher temperature heat where the vapor is absorbed into a suitable liquid. This absorption process not only transfer the latent heat of the vapor

condensing, but also the (much larger) heat of solution (HOS) of the vapor medium (NH3) dissolving into the liquid (low %NH3 in aqua solution), to the point of absorption, generating higher temperatures. The vapor needed for the absorption process may be generated using different mechanisms, eg. heat generated (boiled off), condensed and pumped as liquid to an evaporator, where additional heat again evaporate the pumped liquid ready for the absorber (typical AHT of figure 3, above). Another way is shown in the Hybrid AHT of figure 4, where a vapor compressor raise the vapor pressure of the heat generated vapor high enough to be ready for the absorber. In this heatpump a large portion of the energy required to produce the vapor is heat absorbed from a cold source (Q_cold) in the desorber, while a smaller portion comes from the electrically driven compressor motor. The electrical efficiency (COP_e) is therefore higher (nearly 10) compared to the standard VC type heat pump (COP_e ~ 3 to 4). The same principles, but slightly different economics were shown in the publication [21] where the Hybrid-AHT is described using an Ejector type Vapor Compressor to replace the standard compressor of the heat pump in figure 4, above.

This current paper try to develop and demonstrate a practical, low cost heat driven Heatpump using the already proven sliding temperature heat exchanger and vapor absorption heating principles.

In this development, the process parameters like temperature, pressure, enthalpy, %NH3 concentration of ammonia in NH3 in aqua mixtures etc. mentioned in this document are provided from lookup tables generated in spreadsheets making use of the Thermophysical Properties of NH3 + H2O solutions information of Conde-Petit [7] published in 2004, Ganesh and Srinivas [8] published January 2011. Thermodynamic Properties of water and steam is from Keenan et al [10] published 1969 and Saturated and superheated Ammonia by Haar and Galager [11] published in 1978.

Current Status of the REHOS Intellectual Property (IP):

The IP protection path started with the Provisional Patent Application # 2016/06959 of priority date 11 October 2016, after which various description papers and explanation documents were being released and published. This was followed up with a PCT Application, PCT/IB2017/056283 dated 11 October 2017. The subsequent International Search results from the PCT Examiner was very encouraging, declaring the REHOS cycle and claims New, Inventive and Industrially Applicable, paving the way for full international patenting.

The Sliding Temperature Heat Exchanger (Bubble Reactor)

The constant pressure, sliding temperature effects of binary mixtures (like NH3 in aqua) media used in heat exchangers of thermodynamic cycles like the Kalina cycle and the Hybrid-AHT cycle sketched in figure 4, above, are well known technology used commercially in many waste heat recovery applications.

Let us have a re-look at such a heat exchanger and look at some characteristics of the vertical, tubular column filled with a mixture of 60% NH3 dissolved in H2O. A vertical pipe from stainless steel (SS-316) was designed as per the information listed in table 1, below. The pipe was (for calculation purposes) divided into 21 imaginary segments, numbered 1 to 21 from top to bottom, and the whole column completely sealed. The column is used later as the heart of a unique absorption heat transformer (AHT), therefore the name given as Bubble Reactor. In this first part of the discussion, the reactor is not tied to anything else, filled with the binary media and sealed completely, and we calculated the effects of heat being added (or removed) from the column. These effects would be verified experimentally, and are well known in the operation of commercial binary heat exchangers.

Table 1

Bubble Column Design		
Column Diameter:	**5.00E-02**	m
Length (Column Height):	**1.00E+00**	m long
Segment Lengths:	**4.76E-02**	m
Segment Volume	**9.35E-05**	m3
Number of Segments	**21**	
Column Total Volume	**1.96E-03**	m3

The ammonia in aqua mixture filling the column have the thermodynamic characteristics as listed in table 2, below, at the ambient temperature of 20°Celsius. When external heat is added (with a blowtorch), some vapor is driven off, rising as bubbles vertically with the following results:

Table 2

Media Uncharged Conditions @ Ambient Temperatures		
Ambient Temp	**20**	Celsius
Media NH3 Concentration	**60.0%**	NH3
Media Saturation Pressure	**4.079E+05**	Pa Abs
Liquid Saturation Density	**729**	kg/m3
Vapor Saturation Density	**17.6**	kg/m3
Media Saturated Liquid Enthalpy	**-1.39E+05**	J/kg
Media Saturated Vapor Enthalpy	**1.13E+06**	J/kg
Media Latent Heat	**1.27E+06**	J/kg
Total Column Media Mass	**1.43E+00**	kg

The two columns in figure 5, below, tell more or less the full story. As the metal tubes are sealed, and completely liquid filled, the NH3 in aqua internal media would be completely in saturation at all positions in the column, and would stay in saturation in all segments. Heat added to a saturated mixture would desorb or boil off, some vapor (with a very high NH3 content, depending on temperature of the liquid). This will instantaneously increase the pressure inside the closed container, creating a slightly subcooled environment, where the vapor generated is then re-absorbed in the mixture, restoring saturation directly above the point of heat entry. The buoyancy of the original vapor bubble generated, would push

upwards and set the liquid in motion like a "vapor lift" pump. Absorption of this vapor bubble generate heat, desorbing more vapor, displacing the heated, lower concentration liquid downwards as it moves upwards. This higher concentration (and lower temperature) vapor/liquid mixture thus migrates vertically upwards, while the denser, hotter lower concentration liquid migrate downwards. A NH3 concentration gradient

Figure 5

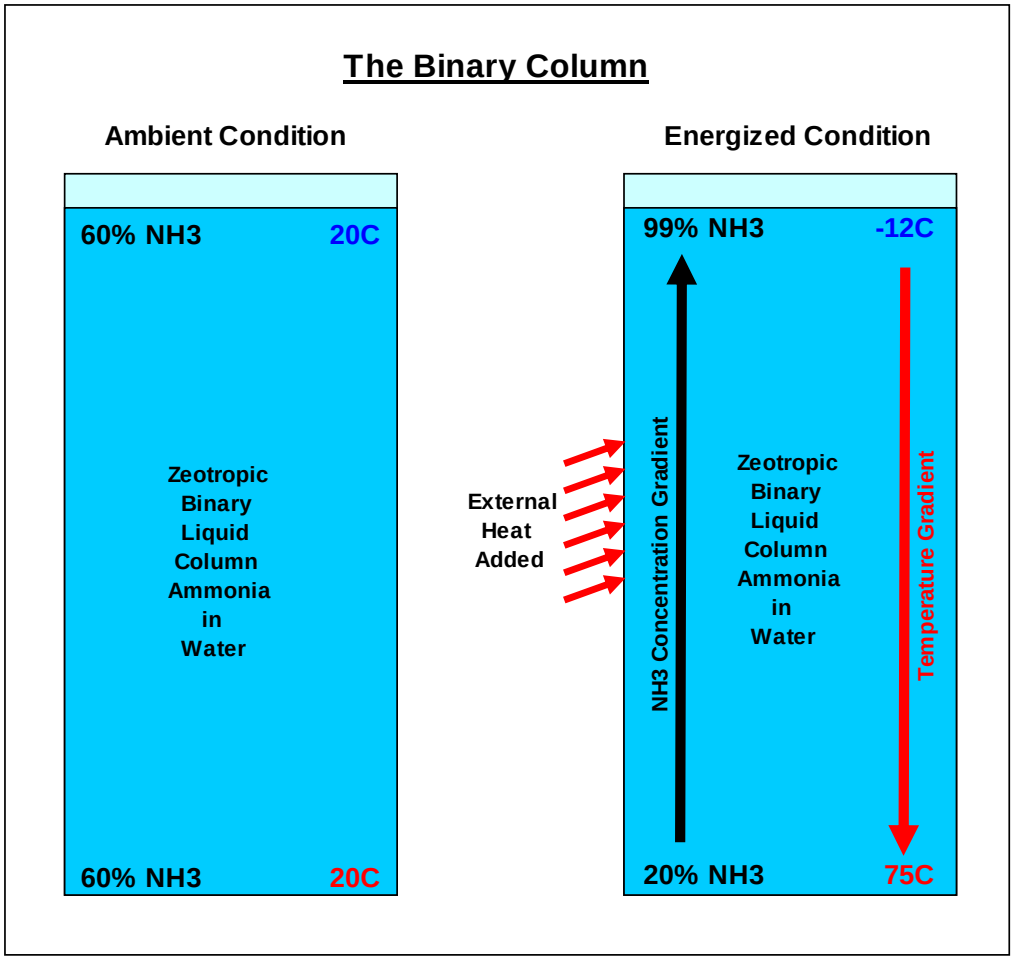

is thus formed with the lowest concentration at the bottom of the column and the highest concentration at the top. Similarly the temperature gradient would see the highest temperature at the bottom of the column and the lowest at the top. While this migration take place dynamically, the column is at a higher dynamic pressure, but as the movement of liquid cease, with the gradients set up, the pressure decrease to a stable "charged" state. The actual value of this dynamic pressure would depend on the rate of heat addition to the column, but for calculation purposes we assumed the pressure would stay close to the original pressure at ambient temperature. During all this internal movements, heat-, mass-, and species transfer take place along the length of the column, but all the segments are essentially at the same (saturation) pressure, while the %NH3 and temperatures change, depending on the specific segment position in the column. We assumed the distribution of NH3 concentration in the different segments would be a linear relation (see graph 2).

The slope of this line would be a function of the amount of external heat added to the column.

The graphical information below reflect the state in each of the 21 segments in both the dynamic and "charged" state.

Graph 1

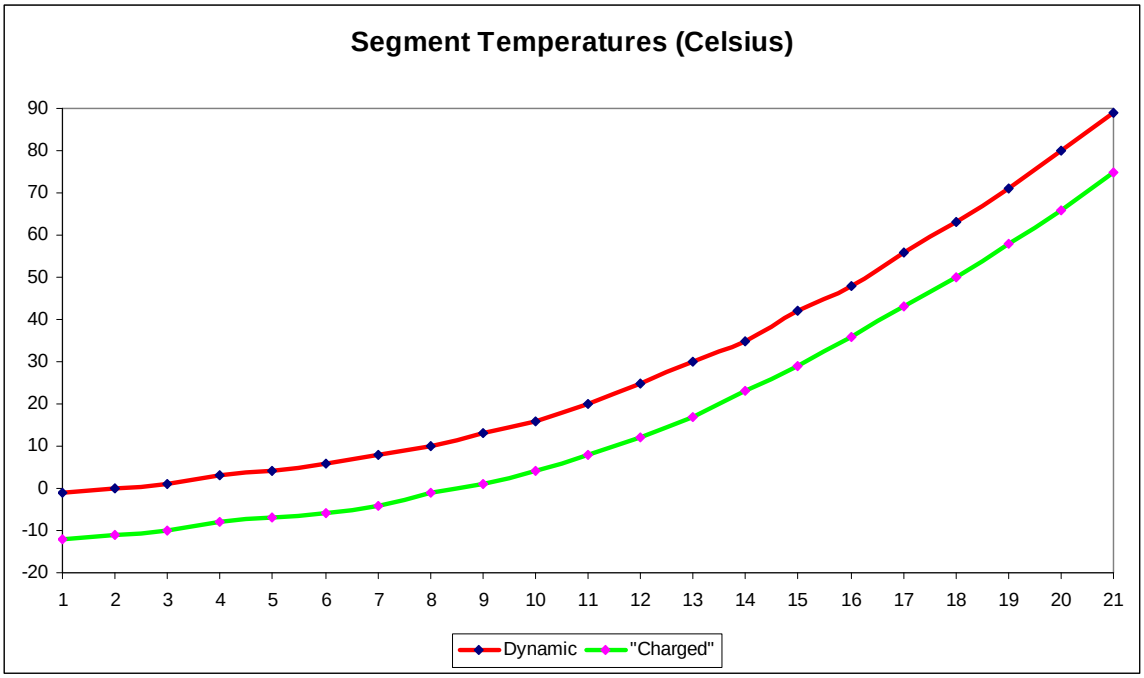

Graph 2

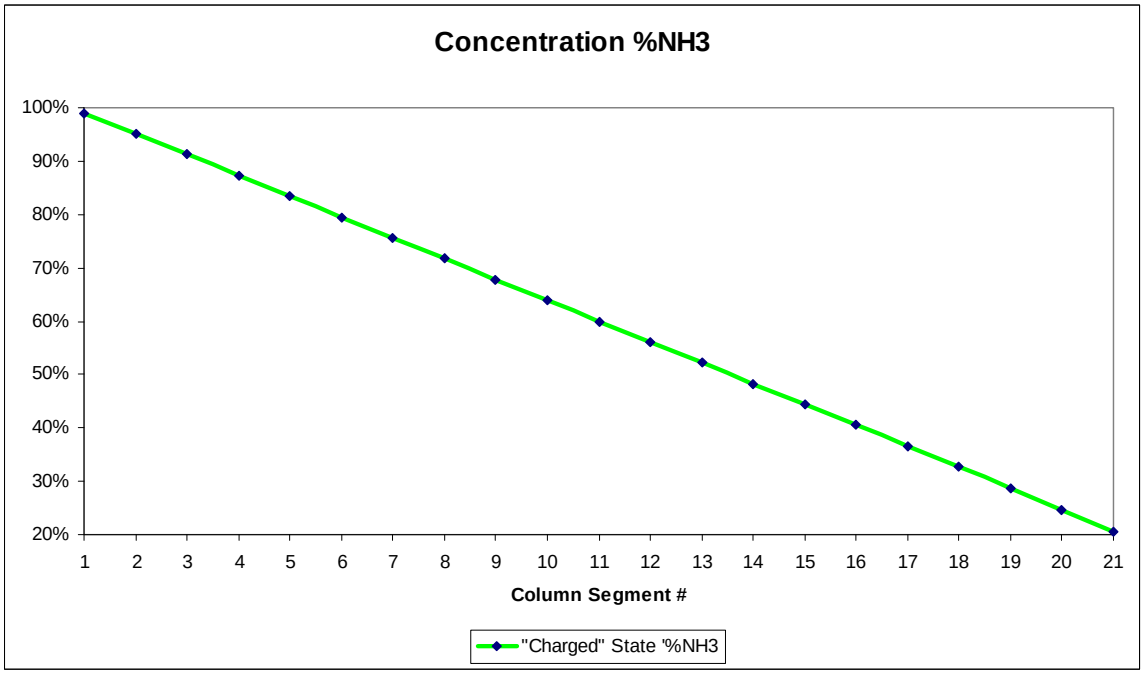

The temperature decrease as liquid move vertically upwards from the low %NH3 at segment 21 to the much higher concentration at segment 1 at the reactor top is a logic consequence of the endothermic dissociation of the binary mixture.

Graph 3

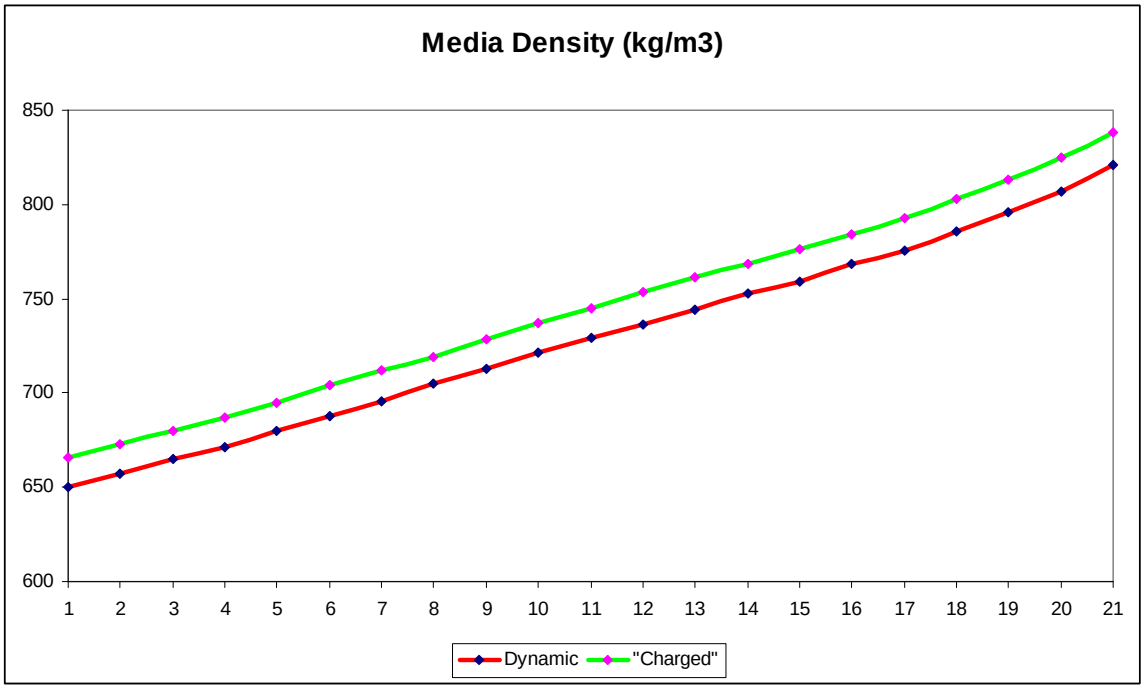

Graph 4

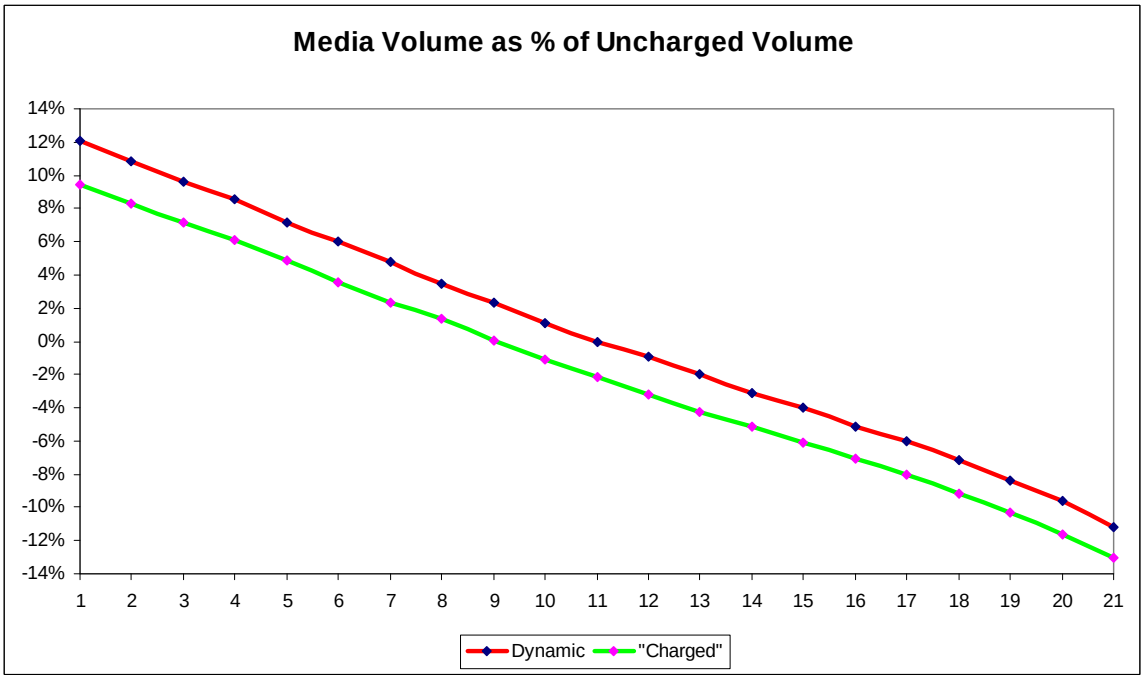

Graph 5

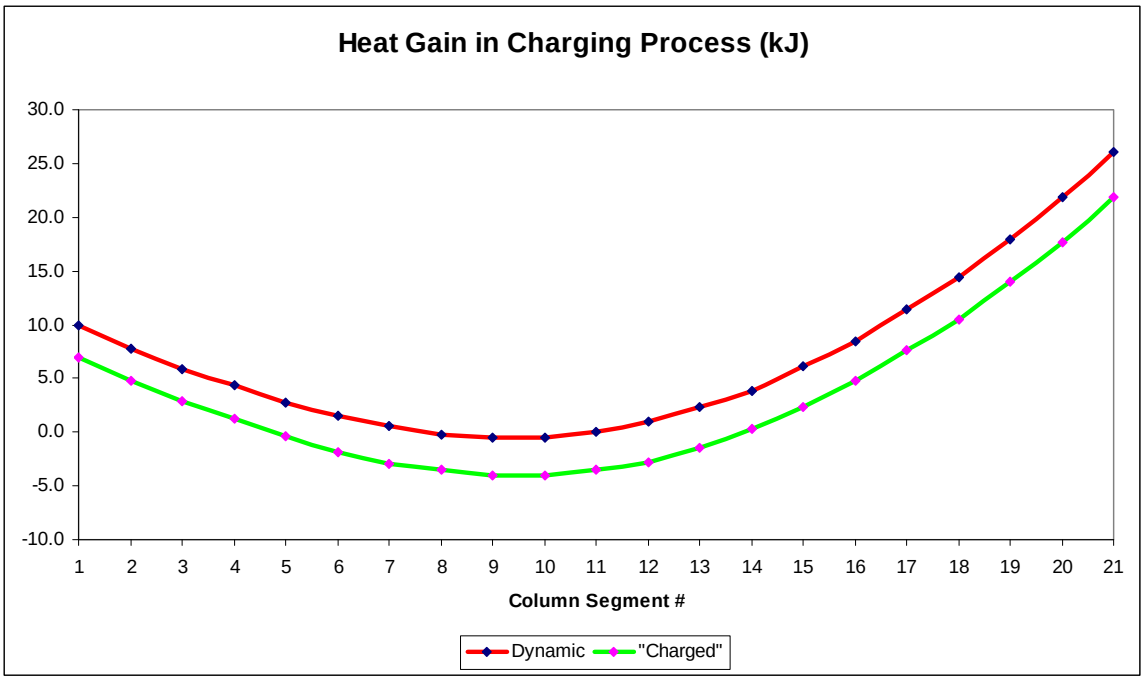

Graph 6

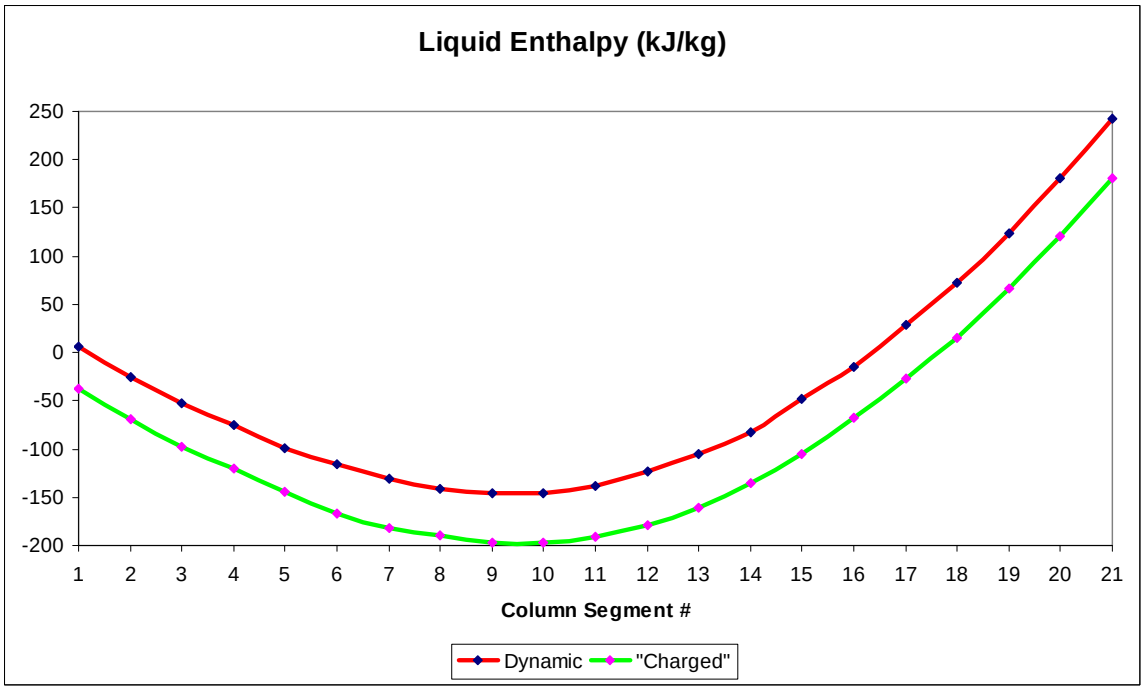

Graph 7

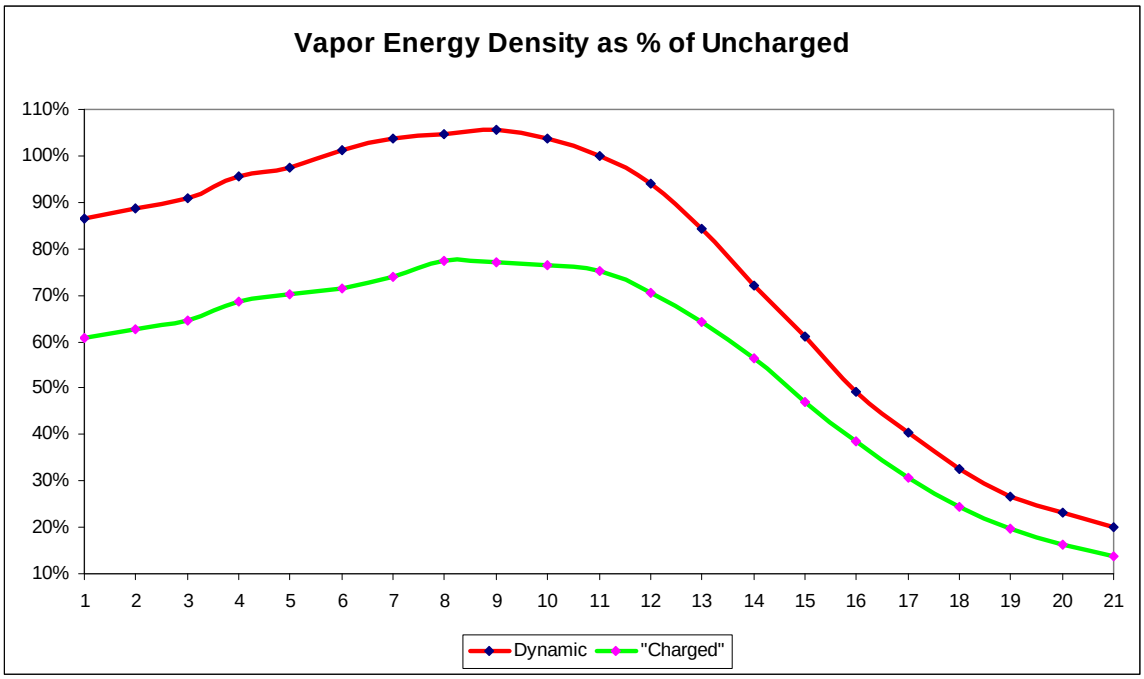

The density shown in graph 3 highlight to us that the "charged" condition would be a stable condition, blocking any convection liquid flows, as the hot bottom liquid in segment 21 has a much higher density than the cold top of the column in segment 1. This implies that the column would actually store the external heat in the gradients formed, and this heat would only be very slowly dissipate due to vertical conduction and radiant heat loss from the heated column.

Table 3

Average Change from Dynamic to "Charged" Condition		
Dynamic (not settled) Pressure	**4.079E+05**	Pa Abs
Charged (stable settled) Pressure	**2.686E+05**	Pa Abs
Pressure Decrease	**34.2%**	
Temperature Decrease	**12.2**	Celsius
Liquid Volume Decrease	**2.2%**	
Liquid Density Increase	**16.3**	kg/m3
Media Enthalpy Decrease	**52065**	J/kg
Heat Removed	**3549**	Joule
Vapor Energy Density Decrease	**20.1%**	

Notice from table 3 that the pressure drop substantially (34%), from the original saturated vapor pressure at ambient temperature, which we took to be the same as the dynamic pressure in the column while the gradients are established. This is of course brought about by heat removal dropping the temperature of all segments by an average of 12,2°C.

Heat added to a sealed column like this create temperature- and NH3 concentration gradients as clearly shown in graph 1 and 2. As these gradients are created by the internal media movements with heat-, mass-, and species transfer, it should be clear that the heat input point is not important, as the same gradients would be created irrespective of where along the column length the external heat input occur! Liquid move both upwards and downwards during this gradient establishment, so it is important that the column diameter is large enough so as not to restrict liquid movement in this counter current flows. Also of significance is the fact that heat is added to the column at a higher temperature (it may be at a temperature above ambient), yet it cools the top of the column to below ambient! Segment 1 slowly cool to -12°C (assuming no ambient heat influence the cold column top).

Table 4

Change from "Uncharged" to "Charged" Condition		
Average Charged Liquid Enthalpy Gain	**5.632E+04**	J/kg per dT = 100C
Average Dynamic Liquid Enthalpy Gain	**1.162E+05**	J/kg per dT = 100C
Liquid Volume Increase	**-1.8%**	

With the creation of these gradients, the enthalpy of the heated column bottom (segment 21), increase to 181 kJ/kg while the cooled column top decrease to -37 kJ/kg, giving the total column range ~ 218 kJ/kg from bottom to top. The amount of energy required for these gradients to be created is actually much less than this, as seen from table 4, above. During the dynamic creation phase while the internal media is still in motion, the average enthalpy gain of the complete column is 116 kJ/kg, which is further reduced to 56 kJ/kg once the gradients have been established. This has a major impact in heatpump development shown later in this document. If liquid is extracted from the column top and injected at the bottom, the high concentration liquid would flow internally from the injection point to the column top, partially destroying the temperature and concentration gradients, unless the additional energy of (at least) 56 kJ/kg is added to the liquid prior to injection. This 56 kJ/kg therefore represent the heat of gradient creation.

Also of significance is the fact that the total liquid volume decrease (by some 1,8%) with a decrease in temperature (and heat content), suggesting that a percentage liquid will flash into vapor to fill this volume decrease within the sealed fixed container volume during heat removal. The generated vapor bubbles would therefore rise to the top, creating internal circulation that would essentially re-define the established gradients and re-distribute the remaining internal energy. Heat loss out of the column would in other words cause a partial gradient destruction, as much as a heat addition would cause a gradient creation. The magnitude of established temperature and NH3 concentration gradients is a direct function of the internal energy in the column media. Should this energy by supplemented with external heat addition, the magnitude of the gradients would increase, while it would decrease on heat loss out of the column.

The saturation vapor have a very interesting energy density characteristic, as shown in graph 7. The vapor energy density at the higher temperatures (>50°C) of the column bottom is less than 30% of the original, "uncharged" saturated vapor energy density. This

enhances bubble formation and greatly increase bubble buoyancy liquid circulation drive (heat transfer in exchanger configuration) at the higher temperature area's in the column, compared to the colder top area. This enhanced heat exchange in the high temperature area and retarded circulation in the cold top area of the column is very useful when designing a heatpump.

The sealed binary column reactor described above may be used as an absorber, economiser and desorber combination of the AHT of figure 4, but with a very much reduced pressure differential. The pressure difference between the absorber and desorber in figure 4 calculate to 13,5 Bar, while the pressure differential of the described binary reactor is only the hydraulic gravity-induced pressure of the liquid column, and for a very small column height (eg. the 1 meter example described) the dP may be as low as 8 kPa while the saturation pressure of the binary mixture is ~ 4 Bar Abs. The dP is therefore negligible small (~ 2%) compared to the saturation pressure in the reactor.

Developing the low dP Bubble Reactor Heat Transformer

Should we use the described reactor column in an AHT, it would look like the sketch

Figure 6

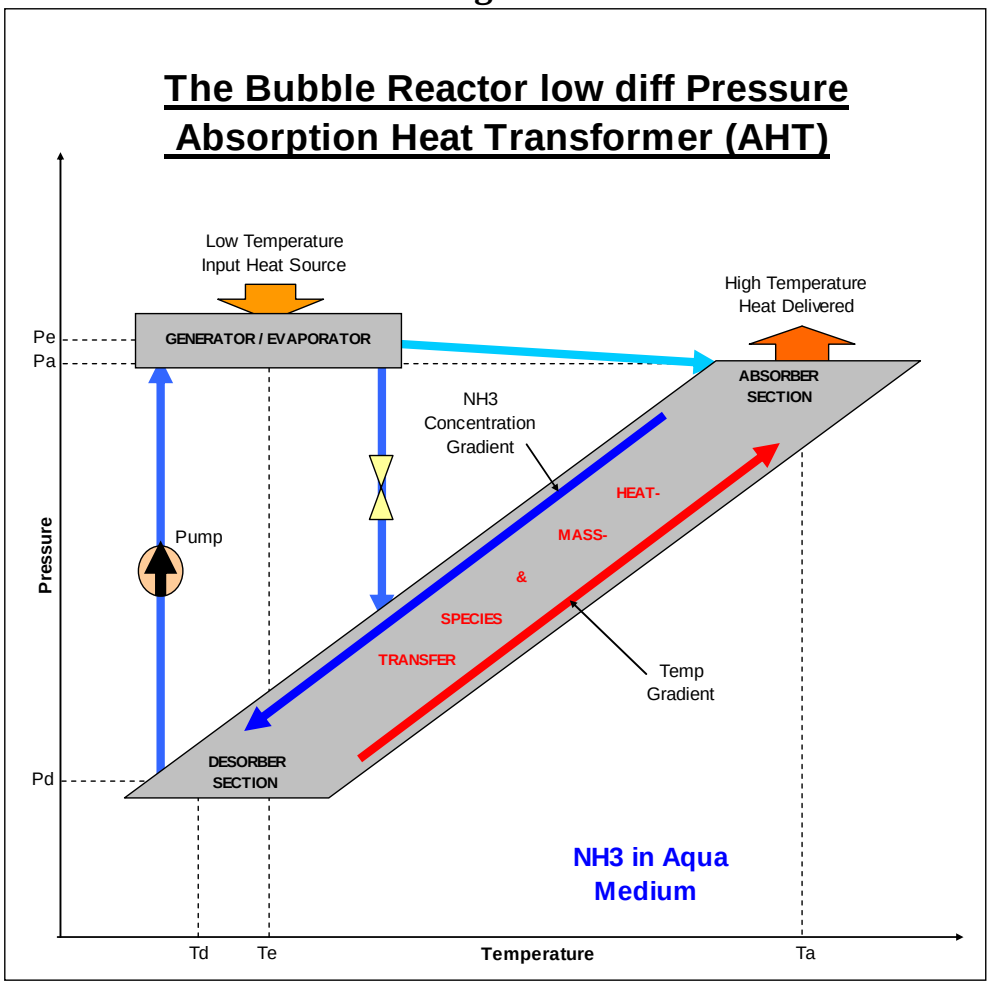

in figure 6, above. The pressures (Pa) and (Pd) differ by only the liquid column (reactor) height gravity induced pressure, so the liquid pump shown may easily be a gravity powered syphon pump, as the required pump output pressure (Pe) is not very high. The temperature (Td) is the reactor cold top temperature and the evaporator temperature (Te) is only 1°C higher than the reactor top, with the evaporator saturation pressure (Pe) only slightly higher than the absorber pressure (Pa) to allow vapor to flow from evaporator to absorber without the need of any compressor.

In a very practical design of the Syphon Bubble Reactor Heat Transformer (Syphon-BRHT) an electrical pump is added for easier starting of the heat driven heatpump. This is shown in the diagram of figure 7, below.

Figure 7

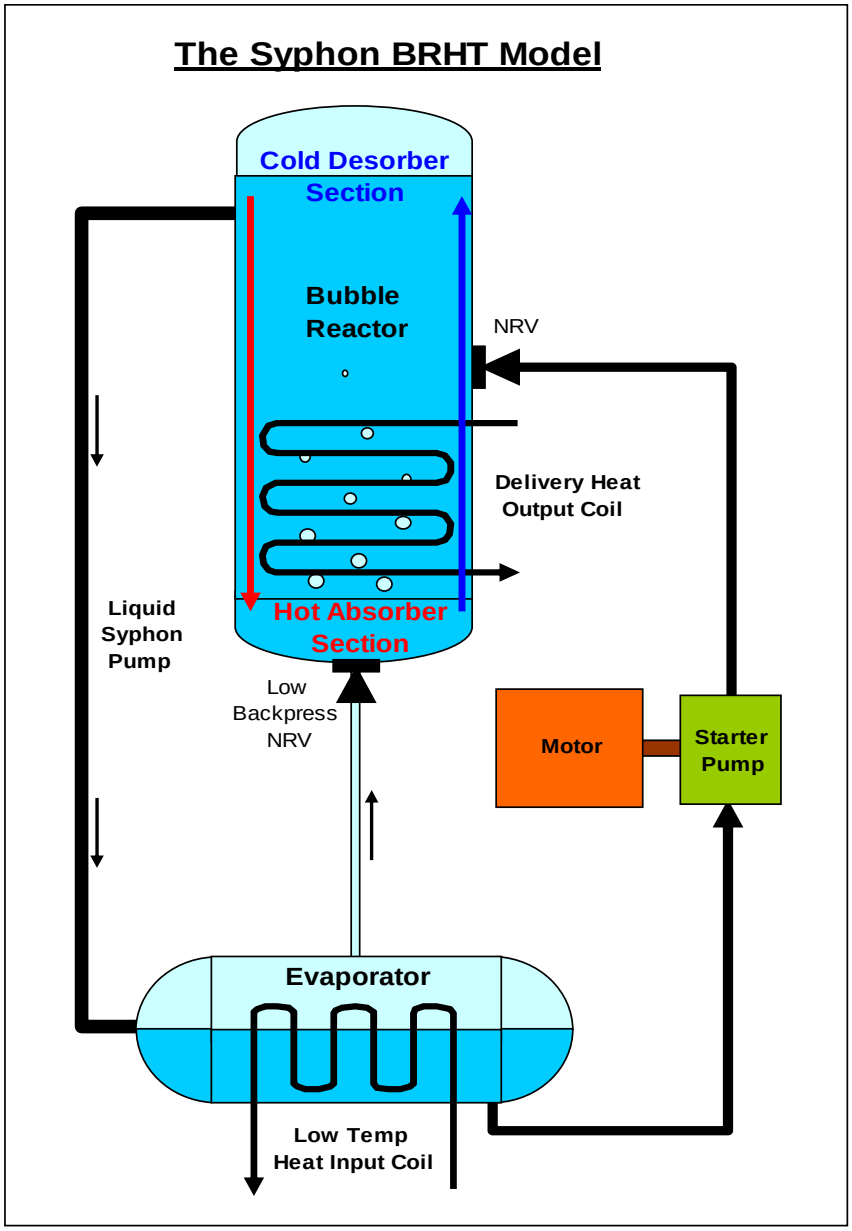

The complete design of this novel Syphon-BRHT heatpump is attached as appendix A to this document. A model as per this design heat pump is in the process of being constructed as proof-of-concept model.

During operation the bubble reactor is kept vertical and behave very similar to the description of the vertical binary column in the first part of this paper, with the temperature and ammonia concentration gradients established. Low temperature (-9°C) NH3 in aqua concentration @ 98,56%NH3 saturated binary liquid enter the syphon pump and the pressure is increased by gravity as the liquid flow to the horizontal evaporator. The liquid level in the evaporator and the bubble reactor differ in vertical height by 2,11 meters, making sure the vapor generated in the evaporator is at the elevated pressure high enough to balance the liquid reactor column hydraulic pressure as it flows from the evaporator into the reactor via the low dP non-return valve (NRV). This NRV was spring-loaded, but the spring have been removed to reduce the required differential pressure to open the NRV. It is kept closed by liquid column hydraulic pressure.

As evaporator pressure is generated by the syphon pump, any evaporator liquid overflow would have to be pumped vertically upwards against gravity, and we have therefore added the "Starter" pump for this purpose. When the machine just start up, all the NH3 and water is still mixed uniformly and the complete evaporator and piping are all filled with this mixture. Heat provided into the evaporator heat exchange coil will boil off some vapor (essentially pure NH3) that would fill the upper side of the evaporator and the vapor delivery tube and start pushing into the bubble reactor. At this early starting stage, the evaporator would perform more the function of vapor generator, boiling off NH3 as vapor, but leaving behind the lower %NH3 liquid mixture that need to be pumped by the starting pump back to the bubble reactor. As the system warm up, the bubbles being absorbed in the bottom area of the reactor generate heat, initially creating the temperature and concentration gradients as described before. During this starting phase, the starting pump have a large mass flow, but as the gradients are reaching design point, the liquid leaving the reactor via the syphon pump becomes higher and higher concentration NH3, so the requirement for pumping the evaporator spill-over becomes less as an increasing percentage of the liquid entering the evaporator is actually evaporated. At the design point the starter pump mass flow is only about double the evaporated vapor flow and the starter pump just idles along.

During start-up the cold temperature of the reactor top created by the temperature gradient as explained before, gradually decrease the temperature of the syphon pumped liquid and therefore also the evaporator, so the heat absorption from the starting heat source by the evaporator increase while the evaporator saturation temperature decrease, until the design point is reached, where the evaporator operate on a temperature of ~ -8°C and the bubble reactor top is at about -9°C.

The heat output coil remove high temperature heat from the reactor bottom (at 80°C design point), but should also balance the heat flow in the system. Should the heat input into the system (the evaporator), be greater than the heat removal by the delivery heat output heat exchanger coil from the bubble reactor bottom, the gradients would be

increased in magnitude, while gradient destruction would take place when the heat Nett inflow into the system decrease. At design point the heat absorbed into the evaporator would be ~ 10 kW_th while the heat delivery would reach ~ 97% of that, the balance lost as conduction and radiated heat loss (some 300 W estimated as worse case), from the imperfect thermal insulation of the bubble reactor. The 482 Watt required as the heat of desorption only influence the charging (starting) phase, as operation at design point is calculated with heat-, mass-, and species balance of each segment of the reactor. This low (482 W is only 4,8% of the evaporator heat load) energy requirement stems from the low desorption heat (56 kJ/kg) as described on page 13 above.

In this Syphon-BRHT design it is foreseen that the complete bubble reactor, evaporator and all piping would be thermally insulated so that heat input and output only occur via the heat exchanger piping liquid flow.

As heatpump for upgrading waste heat (eg. Solar Pond) this design would deliver a thermal efficiency (COP_th = 0,97) while it used very little electricity and the starter pump at operational design point would use only ~ 7,88 Watt, while the heat transformer deliver close to 10 kW_th. The electrical efficiency (COP_e = 1232) being in excess of 1000 is therefore no surprise, and commercially valued extremely high.

The utilization of this type of Syphon-BRHT heat pump as primary sub-cycle for coupling regeneratively to an ORC to form a REHOS cycle is, however, revolutionary! The results of such a coupling are shown in table 5 below.

Table 5

Possible ORC coupled Regeneratively Performance:			
ORC High Temperature (Reactor Max - 10C)		70	Celsius
	ORC Low Temperature (Evap + 10C)	2	Celsius
	ORC Subcycle Assumed Efficiency	12.1%	(61% Carnot)
REHOS Heat Input (Heatpump Input - ORC Rejection)		1470	Watt
REHOS Power (ORC Power - Pump Power)		1170	Watt
REHOS Cycle Thermodynamic Efficiency		79.6%	

To form the REHOS cycle, the ORC evaporator would be the heat delivery output coil positioned in the bottom of the bubble reactor, and operating on 70°C, which is some 10°C lower than the actual bubble reactor bottom liquid temperature to allow for good heat transfer. The ORC condensing (heat rejection) coil would be placed inside the evaporator, adjacent to the existing evaporator environmental heat input exchanger coil, so the ORC low pressure condensing can take place at 2°C, which is 10°C higher (for proper heat exchange), than the evaporator saturation temperature of -8°C. The ORC would realistically operate on 61,25% Carnot efficiency (12,1%), brought about by using NH3 as medium with a turbine delivering 75% isentropic efficiency. This way the overall heat balance would be short of ~ 1470 Watt, which must be supplied from external

means. The ORC heat rejection deliver the balance of the 10 kW_th waste heat load to the evaporator. **This REHOS configuration would realistically provide power at 79,6% thermodynamic efficiency, from waste heat at a temperature ~ ambient! More carefull design of the ORC, with closer heat exchanger approach temperatures and a higher efficiency turbine would push this REHOS efficiency to values > 80%. It represent the highest thermodynamic efficiency of any heat engine known to man!**

References:

1. Hybrid Heat Pump for Waste Heat Recovery in Norwegian Food Industry, Stein Rune Nordtvedt, Institute for Energy Technology, Instituttveien 18, N-2027 Kjeller Bjarne R. Horntvedt, Hybrid Energy AS, Ole Deviks vei 4, N-0666 Oslo, Jan Eikefjord, John Johansen, Nortura AS, Rudshøgda, Norway, Stein.Nordtvedt@ife.no. *(This paper was published in the proceedings of the 10th International Heat Pump Conference 2011.)*. This paper is also published as part of the IEA Handbook [2], page 57 - 61.

2. Thermally driven heat pumps for heating and cooling, compiled and edited by Annette Kühn (Ed.) as the Universitätsverlag der TU Berlin 2013, as the IEA Handbook available as handbook ISBN (online) 978-3-7983-2596-8 at email publikationen@ub.tu-berlin.de

3. Experimental Evaluation of a single-stage Heat Transformer used to increase Solar Pond's Temperature, by W. Rivera of Centro de Investigación en Energia-UNAM, P.O. Box 34, 62580, Temixco, Mor. , Mexoco and published in Solar Energy Vol 69, No. 5, pp. 369 - 376, 2000.

4. Industrial Heat Pumps for High Temperature Process Applications *(A numerical study of the ammonia-water hybrid absorption-compression heat pump)* by Jonas Kjaer Jensen, Ph.D. Thesis, Kongens Lyngby December 2015, DTU Mechanical Engineering, Technical University of Denmark.

5. Development of the Hybrid Absorption Heat Pump Process at High Temperature Operation, by Anders Borgås, Masters Thesis June 2014, NTNU Department of Energy and Process Engineering, Norwegian University of Science and Technology.

6. An Introduction to the Kalina Cycle, reprinted by Henry A. Mlcak, PE , first published in PWR- Vol.30, Proceedings of the International Joint Power Generation Conference, with editors: L. Kielasa and G.E. Weed, Book No. H01077-1996.

7. Thermophysical Properties of NH3 + H2O solutions for the industrial design of absorption refrigeration equipment, by Dr Manuel R. Conde-Petit (M. Conde Engineering, Zurich - Switzerland) 2004.

8. Evaluation of thermodynamic properties of ammonia-water mixture up to 100 bar for power application systems, by N. Shankar Ganesh and T. Srinivas of the Vellore Institute of Technology, Vellore-632014, India. This paper was published in Journal of Mechanical Engineering Research Vol. 3. (1), pp. 25-39, January, 2011.

9. Analysis of Absorber Operations for the 5 kW Ammonia/Water Combined Cycle by Sirisha Devi Govindaraju as Thesis Presented to the Graduate School of the University of Florida in Partial Fulfillment of the requirements for the Degree of Master of Science, 2005.

10. Thermodynamic Properties of Water including Vapor, Liquid and Solid Phases, by J.H. Keenan, F.G. Keeyes, P.G. Hill, J.G. Moore and published by John Wiley & Sons Inc 1969.

11. Thermodynamic Properties of Ammonia by Lester Haar and John S. Gallager, published in J. Phys. Chem. Ref. Data, Vol. 7, No. 3, 1978.

Previous Publications:

12. Paper presented at PowerGen Africa Conference July 2017 and published in the conference proceedings titled "Introducing a novel thermodynamic cycle (patent pending), for the economic power generation from recovered heat pumped from the huge global thermal energy reservoir called earth" by Johan Enslin, Heat Recovery Micro System CC. This paper is also accessible from my website http://www.heatrecovery.co.za/.cm4all/iproc.php/PowerGen-Africa 2017 Proceedings Speaker0_Session19149_1.pdf

13. A Paper titled "The Simplified REHOS Cycle.pdf" was written by Johan Enslin in August 2017 and published on my website http://www.heatrecovery.co.za/.cm4all/iproc.php/The Simplified REHOS Cycle.pdf

14. A Paper titled "Clarifying Process Parameters for the REHOS Cycle Concept_rev3.pdf" was written by Johan Enslin in October 2017 and published on my website http://www.heatrecovery.co.za/.cm4all/iproc.php/Clarifying Process Parameters for the REHOS Cycle Concept_rev3.pdf

15. The Paper titled "The Binary NH3-H2O Bubble Reactor_rev1.pdf" was written by Johan Enslin in December 2017, and published on my website http://www.heatrecovery.co.za/.cm4all/iproc.php/The Binary NH3-H2O Bubble Reactor_rev1.pdf

16. The Paper titled "The Competitive Advantages of REHOS Technology_rev1.pdf" was compiled by Johan Enslin in early January 2018, and published on my website http://www.heatrecovery.co.za/.cm4all/iproc.php/Competitive Advantages of REHOS Technology_rev1.pdf

17. Another paper, "Executive Overview of the REHOS Technology_rev1.pdf" was compiled by Johan Enslin in February 2018 and published on my website http://www.heatrecovery.co.za/.cm4all/iproc.php/Executive Overview of the REHOS Technology_rev1.pdf

18. The follow-up document "Clarification of COP calculations for Absorption Heat Transformer (AHT) Type Heat Pumps.pdf" was written by Johan Enslin (to enhance the Executive Overview paper) in March 2018 and published on my website http://www.heatrecovery.co.za/.cm4all/iproc.php/Clarification of COP calculations for Absorption Heat Transformer (AHT) Type Heat Pumps.pdf

19. The document titled "Comparison of various Modern Heatpump Technologies for unlocking Commercial Value from Ambient Heat_rev4.pdf" was written by Johan Enslin in April 2018 and published on my website http://www.heatrecovery.co.za/.cm4all/iproc.php/Comparison of various Modern Heatpump Technologies for unlocking Commercial Value from Ambient Heat_rev4.pdf

20. The document titled "Executive Overview of the REHOS Technology Redone April 2018.pdf" was written by Johan Enslin in April 2018 and published on my website http://www.heatrecovery.co.za/.cm4all/iproc.php/Executive Overview of the REHOS Technology Redone April 2018.pdf

21. The document titled "The Proof-of-Concept Model of the REHOS Ejector Heat Pump Part 1.pdf" was written by Johan Enslin in April 2018 and published on my website http://www.heatrecovery.co.za/.cm4all/iproc.php/The Proof-of-Concept Model of the REHOS Ejector Heat Pump_Part 1.pdf

22. The document titled "Competitive Advantages of REHOS Technology_rev2.pdf" was written by Johan Enslin in April 2018 and published on my website http://www.heatrecovery.co.za/.cm4all/iproc.php/Competitive Advantages of REHOS Technology_rev2.pdf

23. The document titled "REHOS Technology Executive Summary.pdf" was written by Johan Enslin in April 2018 and published on my website http://www.heatrecovery.co.za/.cm4all/iproc.php/REHOS Technology Executive Summary.pdf

24. Website for Heat Recovery Micro Systems where the above publications are available from: www.heatrecovery.co.za

Appendix A

Table A1

Downcomer Syphon Pump Design			
Downflow Mixture Bulk Temperature	**-9**	Celsius	
H/E Coil Tube ID	**8.00E-03**	m	
Downcomer Mixture Flow Velocity	**0.8**	m/s	
Re	**21677**		
Friction factor f	**0.0256**		
Tube Length	**2.11**	m	
Tubing Pressure Drop	**1.39E+03**	Pa	

Table A2

Evaporator H/E Coil Design			
Tube Wall Temperature	**0**	Celsius	
H/E Coil Inlet Water Bulk Temperature	**22**	Celsius	
Chilled Water Outlet Temperature	**3**	Celsius	
H/E Coil Tube ID	**8.00E-03**	m	
Evaporator H/E Water Mass Flow	**1.25E-01**	kg/s	
Evaporator Coil Water Velocity	**2.5**	m/s	
Re	**15482**		
Pr	**9.3**		
Friction factor f	**0.0279**		
f_adjusted	**0.0324**		
Nu	**145.2**		
Nu_adjusted	**124.2**		
h	**8996**	W/m2.K	
Tube Length	**5.0**	m	
H/E Area	**1.26E-01**	m2	
LMTD	**9.5**	Celsius	
Heat Transferred	**10780**	Watt	
Tubing Water Flow Pressure Drop	**6.34E+04**	Pa	

Table A3

Reactor H/E Coil Design			
Tube Wall Temperature	**70**	Celsius	
H/E Coil Inlet Water Bulk Temperature	**3**	Celsius	
Hot Water Outlet Temperature	**65**	Celsius	
H/E Coil Tube ID	**8.00E-03**	m	
Delivery Heat H/E Water Mass Flow	**3.73E-02**	kg/s	
Fraction of Chilled Water	**29.7%**		
Evap Coil Water Velocity	**0.8**	m/s	
Re	**5820**		
Pr	**7.1**		
Friction factor f	**0.0368**		
f_adjusted	**0.0273**		
Nu	**39.0**		
Nu_adjusted	**43.2**		
h	**3283**	W/m2.K	
Tube Length	**5.0**	m	
H/E Area	**1.26E-01**	m2	
LMTD	**23.9**	Celsius	
Heat Transferred	**9857**	Watt	
Tubing Pressure Drop	**4.84E+03**	Pa	

Table A4

Bubble Reactor Design		
Vapor Flowspeed in Riser Tube	**13.92**	m/s (Max)
Bubble Reactor 5" ID	**1.35E-01**	m
Bubble Reactor Height	**7.00E-01**	m
Bubble Reactor Mixture Volume	**9.95E-03**	m3
Syphon Pump Liquid Volume	**1.06E-04**	m3
Bubble Vapor Feed Tube Volume	**6.81E-05**	m3
Average Contents Density in Reactor	**562**	kg/m3
Bubble Feed Tube Length	**1.36E+00**	m @ Design Point
Liquid Mass in Reactor	**5.59E+00**	kg
Liquid Mass in Syphon Tube	**7.01E-02**	kg
Liquid Mass in Starter Pump & Tube	**7.01E-02**	kg
Vapor Mass in Bubble Feed Tube	**8.52E-04**	kg

Table A5

Evaporator & Starter Pump Design		
Evaporator Body 4" ID	**1.082E-01**	m
Evaporator Body 4" Length	**6.000E-01**	m
Evap Liquid Volume (50% of Total)	**2.76E-03**	m3 @ Design Point
Evap Vapor Volume (50% of Total)	**2.76E-03**	m3 @ Design Point
Starter Pump Liquid Lines Volume	**1.06E-04**	m3 @ Design Point
Liquid Mass in Evaporator	**1.83E+00**	kg
Vapor Mass in Evaporator	**3.45E-02**	kg
Starter Pump Assumed Efficiency	**35%**	Isentropic
Starter Pump Mass Flow Factor	**2.0**	Factor of Bubble Vapor Flow
Start Pump Overpressure	**9.37E+04**	Pa (for NRV backpressure)

Table A6

Syphon BRHT Heat Pump Process Parameters @ Design Pont						
Position	**Temperature (Celsius)**	**Pressure (Pa Abs)**	**%NH3**	**Mass Flow (kg/s)**	**Enthalpy (J/kg)**	**Energy Flow (Watt)**
Bubble Reactor Top	**-9**	**3.000E+05**	**98.56%**		**-2.94E+04**	
Bubble Reactor Bottom	**80**	**3.053E+05**	**20.01%**		**2.06E+05**	
Reactor Bubble Vapor Inlet	**-8**	**3.053E+05**	**98.56%**	**8.75E-03**	**1.106E+06**	
Reactor H/E Coil Inlet	**3**			**3.73E-02**	**1.26E+04**	
Reactor H/E Coil Outlet	**65**			**3.73E-02**	**2.72E+05**	
Liquid Syphon Pump Inlet	**-9**	**3.000E+05**	**98.56%**	**2.625E-02**	**-2.94E+04**	
Liquid Syphon Pump Outlet	**-9**	**3.123E+05**	**98.56%**	**2.625E-02**	**-2.94E+04**	
Evaporator Vapor Outlet	**-8**	**3.123E+05**	**100.00%**	**8.75E-03**	**1.106E+06**	
Evap H/E Coil Inlet	**22**			**1.25E-01**	**9.23E+04**	
Evap H/E Coil Outlet	**3**			**1.25E-01**	**1.26E+04**	
Starter Pump Inlet	**-8**	**3.123E+05**	**98.56%**	**1.75E-02**	**-2.55E+04**	
Stater Pump Outlet	**-8**	**3.955E+05**	**98.56%**	**1.75E-02**	**-2.55E+04**	
Evap H/E Heatload						**10000**
Reactor H/E Heatload						**9700**
Electrical Pump Load						**7.88**
COP_th (providing heat)						**0.97**
COP_e (providing heat)						**1232**

Heat used by Desorption Process inside the Reactor	**482**	Watt
Vapor Bubble absorption Heat as part of Reactor Coil Load	**7876**	Watt
Sensible Heat as part of Reactor Coil Load	**1824**	Watt
Radiation & Conduction Heat Loss from Hot Reactor components	**300**	Watt